Solidification Crack Susceptibility in Weld Metals of Fully Austenitic Stainless Steels (Report II)†

—Effect of Ferrite, P, S, C, Si and Mn on Ductility Properties of Solidification Brittleness—

Yoshiaki ARATA*, Fukuhisa MATSUDA* and Seiji KATAYAMA**

Abstract

The Trans-Varestraint test was carried out to assess the cracking tendency of austenitic weld metals by obtaining the solidification brittleness temperature range (BTR) and ductility curves. The hot crack susceptibility among five types of commercial austenitic stainless steels was compared first of all. The result determined the temperature ranges over which cracking occurred and suggested that austenitic SUS 304 (Japanese Industrial Standard: 18Cr-8Ni type corresponding to AISI 304), etc. containing δ-ferrite were resistant to hot cracking due to the narrow BTR, the large value of the minimum augmented-strain (E_{min}) within BTR and no ductility-dip temperature range (DTR) at all, and that fully austenitic SUS 310S (JIS: 25Cr-20Ni type corresponding to AISI 310S) was the most susceptible to solidification and ductility-dip crackings due to the widest BTR and the smallest value of E_{min} within BTR and DTR. Furthermore, the effects of P and S on the hot crack susceptibility of SUS 304 and SUS 310S and then the effects of Si, Mn and C on the crack susceptibility of 25Cr-20Ni type alloy were studied. The decrease in P and Si contents was the most beneficial at present study to modify fully austenitic stainless steel 25Cr-20Ni type alloy and the addition of about 1% Mn was probably necessary to reduce cracking caused by the detrimental effect of S, as Mn has potency to combine with S. The increase in C content improved the tendency of ductility-dip and the addition of 0.53%C narrowed the BTR and raised the E_{min} within the BTR, therefore the weld metal may be resistant to hot cracking. However, the microstructure showed a considerable amount of eutectics with γ and M_7C_3 carbides.

1. Introduction

It is generally recognized that fully austenitic stainless steel weld metals show greater susceptibility to hot cracking than austenitic ones containing some residual δ-ferrite in the room temperature microstructure. The susceptibility to hot cracking during welding is one disadvantage for the application of fully austenitic stainless steels, and considerable effort has been devoted to its study. For example, the effect of alloy chemistry has been widely investigated by means of various hot cracking tests[1] such as Circular Groove test[2], FISCO test, Murex Hot Crack test[3], Cast Pin Tear test[4),5], Hot Ductility test[6], WRC fissure bend test[7] and Varestraint test[8]. The data of the above-mentioned tests are in general accordance with the results that impurities such as P, S, etc. are the most detrimental and the presence of the residual δ-ferrite is most effective to prevent hot cracking in austenitic stainless steel weld metals. However, the effect of δ-ferrite is not satisfactorily explained, so far. Therefore, in a previous study[9], since hot cracks occur at high temperature[10),11], the authors investigated the solidification process and the effect of primary δ-ferrite on the segregation of the impurities P and S during welding from a metallographic viewpoint, using fully austenitic SUS 310S and duplex austenitic SUS 304. The result indicated that in case of SUS 304 a large amount of δ-ferrite was formed during solidification and reduced the segregation of P and S to grain boundaries in comparison with the primary austenite in SUS 310S weld metal. The purpose of this study was to evaluate quantitatively the effect of the ferrite and the alloying elements P, S, Si, Mn and C on the hot crack susceptibility and to seek after the possibility of modification of chemical compositions which correspond to 25Cr-20Ni type alloys showing fully austenitic microstructure. In this study the Trans-Varestraint test[12),13] which was the most valuable in studying hot cracking at present was carried out to assess the effect of compositional and microstructural variables by comparing the ductility curve of each specimen. The ductility curve could be obtained by this technique.

† Received on April 6, 1977

* Professor

** Graduate student, Osaka University

2. Experimental Procedure

2.1 Materials used

The chemical compositions of materials used are shown in **Table 1**. In the series I tests, five types of commercial austenitic stainless steels were investigated not only to compare the hot crack susceptibility among the types, but also to clarify the relationship between the microstructure and the solidification ductility curve during welding. In the series II and III tests the effect of phosphorus (0.022% to 0.249%) and sulphur (0.004% to 0.22%) contents increased to commercial SUS 304 and SUS 310S used in the previous report[9] were examined. Furthermore, the following chemical compositions were investigated to improve the hot crack susceptibility of fully austenitic SUS 310S. In the series IV tests the effect of decreasing phosphorus content in SUS 310S was investigated. Moreover, the detrimental effect of Si[4),14)] and the beneficial effects of Mn[4),15)] and C[16),17)] were reported by other in-

Table 1 Chemical compositions of materials used

	Materials (SUS)	Composition (wt%)								
		C	Si	Mn	P	S	Cr	Ni	Mo	other
I	304	0.070	0.70	1.18	0.027	0.010	18.26	8.44	0.05	0.05 Cu
	321	0.050	0.89	1.19	0.029	0.011	17.47	9.43		0.31 Ti
	347	0.040	0.61	1.26	0.026	0.007	18.18	9.69		0.62 Nb
	316	0.078	0.53	1.29	0.032	0.013	17.04	11.03	2.27	0.25 Cu
	310S	0.082	0.94	1.58	0.022	0.007	24.66	20.37	0.10	0.04 Cu
II	310S	0.07	0.78	1.08	0.022	0.004	24.40	19.90		0.0361N
	310 P−1	0.06	0.77	1.04	0.055	0.005	23.75	19.55		0.0330N
	310 P−2	0.06	0.79	1.05	0.109	0.003	23.90	19.80		0.0329N
	310 P−3	0.06	0.78	1.02	0.240	0.003	24.10	19.67		0.0332N
	304	0.05	0.63	1.00	0.027	0.004	18.60	9.10		0.0259N
	304 P−1	0.05	0.58	0.94	0.056	0.006	18.50	9.10		0.0264N
	304 P−2	0.06	0.61	0.99	0.121	0.005	18.60	9.10		0.0206N
	304 P−3	0.06	0.60	1.00	0.249	0.005	18.55	9.05		0.0255N
III	310 S−1	0.07	0.73	1.05	0.022	0.017	24.45	19.90		0.0335N
	310 S−2	0.07	0.75	1.03	0.023	0.062	24.40	20.00		0.0323N
	310 S−3	0.06	0.73	1.01	0.023	0.199	24.40	19.95		0.0329N
	304 S−1	0.06	0.60	0.98	0.026	0.023	18.40	9.05		0.0271N
	304 S−2	0.06	0.60	1.00	0.024	0.081	18.80	9.15		0.0285N
	304 S−3	0.05	0.56	0.94	0.025	0.220	18.50	9.10		0.0302N
IV	310S P−1	0.052	0.13	1.36	0.003	0.009	24.68	20.28	0.30	0.002 N
	310S P−2	0.053	0.54	1.33	0.013	0.012	25.05	19.94	0.02	
	310S P−3	0.066	0.66	1.48	0.022	0.007	24.59	20.08	0.03	
	310S P−4	0.066	0.56	1.41	0.032	0.013	24.70	19.86	0.03	
V	310S Si-1	0.071	0.11	1.49	0.006	0.007	24.99	20.08	0.51	0.019 N
	310S Si-2	0.068	0.22	1.46	0.005	0.009	24.99	19.85	0.46	0.017 N
	310S Si-3	0.068	0.31	1.48	0.006	0.007	24.87	19.90	0.48	0.012 N
	310S Si-4	0.067	0.51	1.47	0.007	0.007	24.92	19.97	0.48	0.019 N
	310S Si-5	0.065	0.74	1.55	0.012	0.008	24.85	20.05	0.03	0.06 Cu
	310S Si-6	0.07	1.03	1.44	0.008	0.008	24.84	20.01	0.02	0.02 Cu
VI	310 Mn-1	0.063	0.69	1.15	0.023	0.003	24.60	20.20		
	310 Mn-2	0.065	0.70	1.90	0.022	0.003	25.15	19.90		
	310 Mn-3	0.065	0.70	2.75	0.022	0.003	24.90	19.90		
	310 Mn-4	0.063	0.68	4.70	0.019	0.005	24.55	19.50		
	310 Mn-5	0.063	0.65	6.20	0.021	0.004	24.20	19.30		
	310 Mn-6	0.063	0.70	8.40	0.021	0.005	23.05	18.75		
	310 Mn-7	0.063	0.62	10.5	0.021	0.005	23.45	18.65		
VII	310 C−1	0.07	0.53	0.83	0.022	0.004	25.35	19.80	0.07	
	310 C−2	0.17	0.54	0.84	0.022	0.002	25.85	19.80	0.07	
	310 C−3	0.28	0.58	0.79	0.022	0.003	25.50	19.80	0.07	
	310 C−4	0.43	0.56	0.79	0.022	0.003	25.60	19.70	0.07	
	310 C−5	0.53	0.56	0.82	0.020	0.002	25.60	20.00	0.07	

vestigators. Therefore, the authors examined the effect of the decreasing Si content from about 1 to 0.1% in the series V tests and the effects of the increasing Mn content from about 1 to 10% and the increasing C content from 0.07 to about 0.5% in the series VI and VII tests.

2.2 Experimental procedure

2.2.1 *Trans-Varestraint test*

It is generally accepted that hot cracks which may occur in austenitic weld metals are divided into two types of solidification cracks and ductility-dip cracks based on their temperature of formation[10]. The schematic representation of the ductility curve at high temperature during welding is shown in **Fig. 1**. It

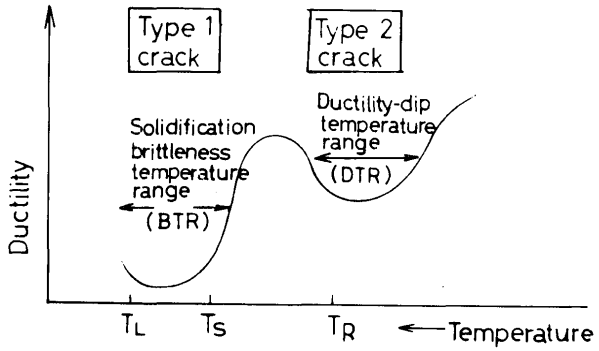

Fig. 1 Schematic representation of ductility curve of weld metal at high temperature.

suggests that low ductility is responsible for hot cracking. The Trans-Varestraint test by which the ductility curve of each alloy during welding can be determined by varying the augmented strain of this technique was used in this investigation. The augmented strain which was applied to the weld metal by substituting a die block with the appropriate radius of curvature and the dropping distance of the yorks was measured by a strain gage and a strain meter, and at the same time the strain rate was measured by an electromagnetic oscilloscope. Since the average strain rate was about 60%/sec in the case of the augmented-strain of 2.5%, the strain was ideally appreciated to be applied almost simultaneously. The specimen in I, IV and V tests were rolled plates of $3\times100\times100$ mm. The specimens in II III were disk plates of about 2.6 mm in thickness and about 110 mm in diameter, and the ones in VI and VII were also disk plates of 3 mm in thickness and about 100 mm in diameter, taken from cast ingots. Each specimen was stuck on a bending block by two bolts at a distance of 70 or 80 mm. The strain was suddenly applied during TIG arc bead-on-plate welding in DCSP conditions of 100A, 12–13V, 150 mm/min (80A for the II and III tests). The maximum length of cracks which occurred in weld metal was directly measured on the as-welded bead surface in the magnification of $\times40$ and $\times16$, and the ductility curve was then obtained by coupling the maximum crack length with the temperature distribution measured with a calibrated W·5%Re-W·26%Re thermocouples (0.3 mm ϕ) immersed in the weld pool during welding. The hot crack susceptibility was evaluated by determining the solidification brittleness temperature range (BTR), the ductility-dip temperature range (DTR), the minimum augmented-strain required to cause cracking (E_{min}) within BTR and DTR and the critical strain rate for a temperature drop (CST) defined as the inclination of the tangent to the ductility curve from the liquidus temperature[13].

2.2.2 *Thermal analysis of alloys*

Each sample was remelted in a crucible in the electric furnace under argon atmosphere, and then the cooling curve was measured with a Pt-Pt-13%Rh thermocouples (PR: 0.5 mm in diameter) and a self-balancing pen-writing recorder. The liquidus temperature (T_L) during not heating but cooling was adopted as the maximum temperature of the BTR. Furthermore, the eutectic melting of segregates such as phosphides in SUS 310S containing 0.05 to 0.24%P, sulphides in SUS 310S and SUS 304 containing about 0.2%S, and carbides in 0.53%C-25Cr-20Ni weld metal were directly observed on a heating cycle by using the hot stage microscope which heating equipment of Mo or W heater could heat a specimen of about $10\times10\times10$ mm cubic at the heating speed of 100 to 1000°C/min.

2.2.3 *Metallographic techniques*

To examine the microstructures of the Trans-Varestraint samples, light microscopy (LM), X-ray diffraction (XD), electon diffraction (ED), and scanning electron microscopy (SEM) with the energy dispersive X-ray spectrometer (EDX) were used. Conventional carbon-extraction replicas were used to investigate the distribution and morphology of inclusions and precipitated phases and to identify them. Furthermore, the residues electrolytically extracted from the weld metals were also identified with the help of XD (Debye-Scherrer and diffractometer methods) and EDX methods.

3. Result and Discussion

3.1 Comparison of hot crack susceptibility of commercial austenitic stainless steel weld metals

The appearances of SUS 310S and SUS 304 weld metals to which an augmented-strain of 3.75% was applied by Trans-Varestraint test are shown in **Fig. 2.**

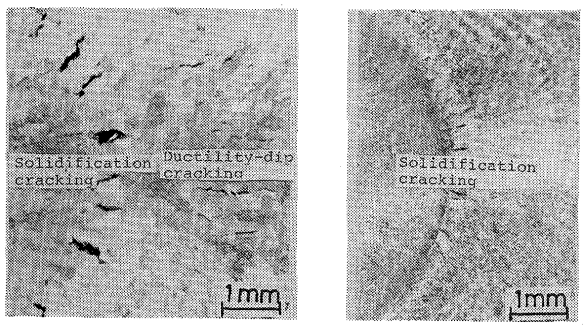

(a) SUS 310S (b) SUS 304

Fig. 2 Appearances of SUS 310S and SUS 304 weld metals at 3.75% augmented-strain by Trans-Varestraint test showing solidification and ductility-dip crackings.

In SUS 310S weld metal two kinds of hot cracking occurred. One is solidification cracking which occurred almost perpendicular to the ripple line that was formed when the strain was applied, and the other is ductility-dip cracking which occurred at lower temperature a little away from the solidification cracks. In SUS 304 weld metal rather smaller solidification cracks occurred but no ductility-dip cracks occurred. It is expected that solidification cracking and ductility-dip cracking occurred within solidification brittleness temperature range (BTR) and ductility-dip temperature range (DTR) respectively shown in Fig. 1. Therefore, the maximum crack length of solidification cracks and the range of occurrence of ductility-dip cracks along the axis of weld metal were measured for each commercial austenitic stainless steel, and subsequently the BTR and the ductility curves at high temperature were determined by coupling the above results with the temperature distribution along the axis of weld metal. The BTR and the ductility curves obtained for five types of commercial austenitic steels are shown in **Fig. 3.** The axes of abscissas and ordinates indicate the temperature and the augmented-strain respectively. The curves of shaded portion show the BTR and the other curves of lower temperature show the DTR. Note that the tendency of the ductility curves which are closely related to the crack susceptibility varies among five types according to the augmented strains. From the result of Fig. 3 the value of the BTR at the augmented-strain of 2.5%, E_{min}, CST was tabulated for each commercial stainless steel

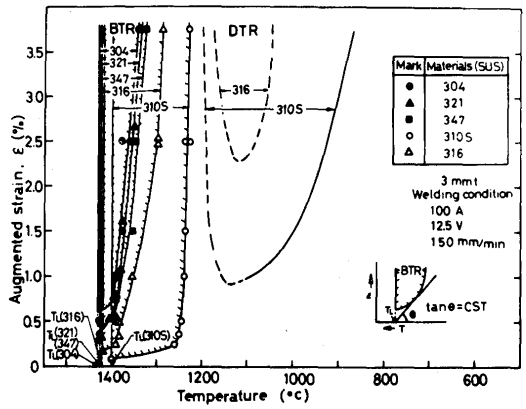

Fig. 3 Solidification ductility curves obtained for five types of commercial austenitic stainless steel weld metals.

Materials (SUS)	BTR (°C)	Emin (%)	CST (%/°C)
310S	170	0.08	0.9×10^{-3}
316	120	0.25	10×10^{-3}
347	80	0.45	16×10^{-3}
321	70	0.4	16×10^{-3}
304	65	0.6	22×10^{-3}

Table 2 BTR at augmented-strain of 2.5%, E_{min} of BTR and CST for commercial austenitic stainless steel weld metals.

in **Table 2.**

SUS 310S exhibited the widest BTR and the lowest E_{min}, and in addition exhibited the susceptibility to ductility-dip cracking within the temperature range from about 1200 to 900°C. SUS 316 exhibited the wider BTR and the lower E_{min}. SUS 304, SUS 321 and SUS 347 exhibited the narrow BTR and the high E_{min}, and moreover did not exhibit the tendency of ductility-dip at all.

The hot crack susceptibility has been discussed from the microstructural viewpoint so far. Therefore, the following refers to the microstructure and the location of formation of hot cracks. The room temperature microstructures from SUS 310S, SUS 316 and SUS 304 weld metals are shown in **Fig. 4 (a)** to **(f)**. In case of SUS 310S, solidification cracks occurred mainly along columnar grain boundaries at higher temperature within the BTR as shown in Fig. 4 (a) and propagated along the migrated grain boundary at the tips of the cracks at lower temperature within the BTR as shown in higher magnification in Fig. 4 (b), and ductility-dip cracks occurred along migrated grain boundaries as shown in higher magnification in Fig. 4 (c) The electron microstructure quenched from about 1100°C during welding, the diffraction pattern from the black particles

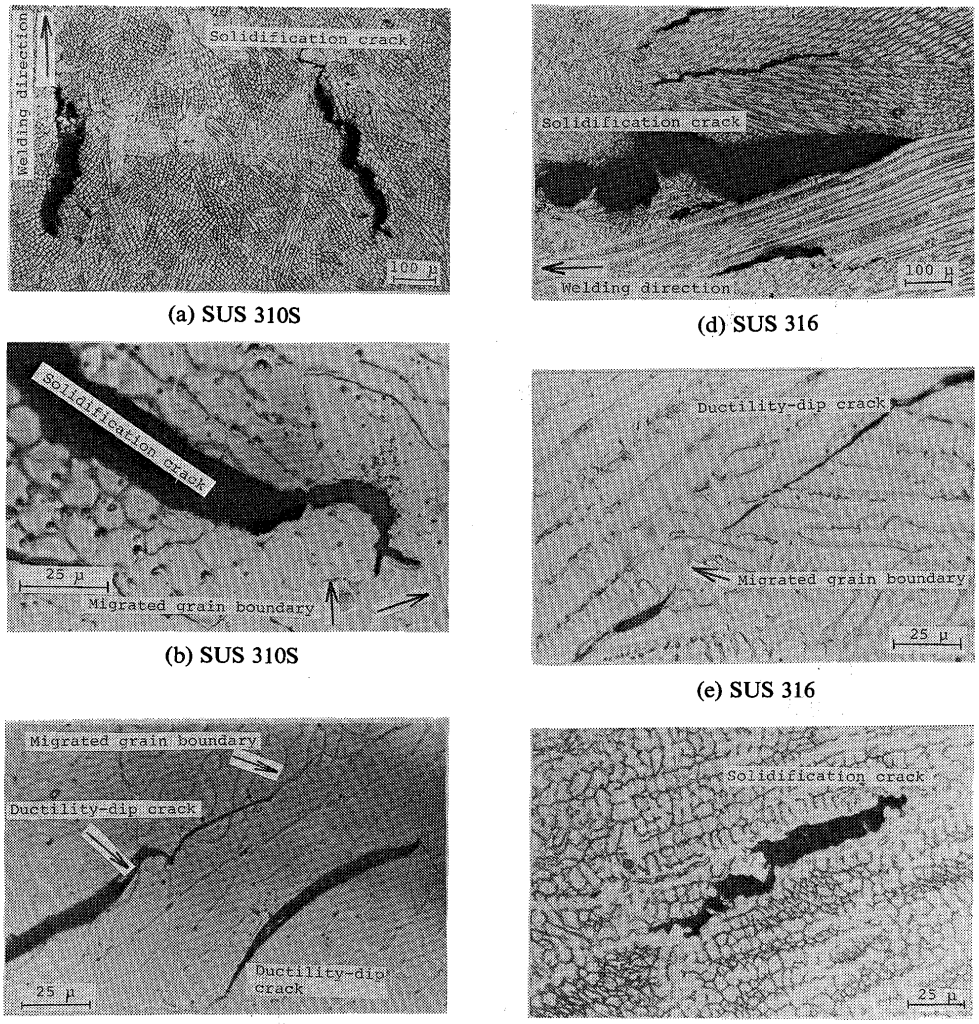

Fig. 4 Room temperature microstructures from SUS 310S, SUS 316 and SUS 304 weld metals showing relationship between microstructure and location of cracks

and its key-diagram are shown in **Fig. 5 (a) (b)** and **(c)**. The microstructure shows that carbides which are identified as $M_{23}C_6$ type (M is predominantly Cr) of a=10.621 A in Fig. 5 (b) and (c) precipitated all over the migrated boundaries. The precipitation of carbides was observed to have been formed along migrated grain boundaries from 1200°C and below and to have hardly been formed in other sites during welding by the electron microscopy. It is taken for granted that the ductility-dip cracking occuring within the DTR was formed along the carbide-precipitating migrated grain boundaries. It is supposed that part of a solidification crack corresponding to the lower temperature within the BTR occurred along a migrated grain boundary not due to ductility-dip cracking but due to the mechanism that it propagated to connect small lakes of liquid enclosed in the solid. It was more clarified from the observation of a crack surface as well as the consideration of the recovery of the ductility

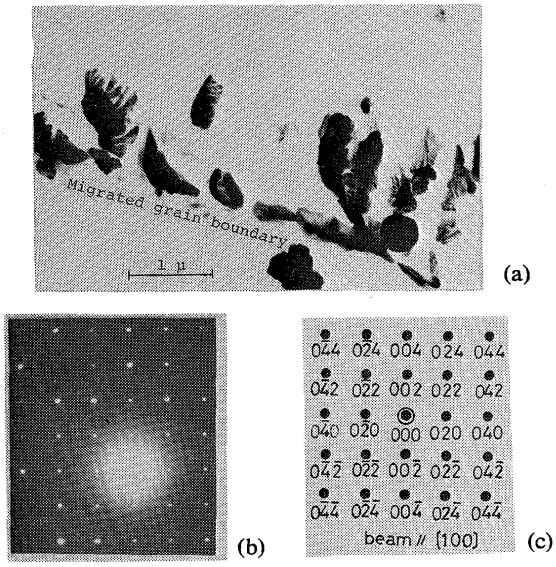

Fig. 5 Electron microstructure quenched from about 1100°C during cooling after solidification showing precipetation of $M_{23}C_6$ carbides identified in (b) and (c) along migrated boundary.

at the lower temperature within the BTR and the existence of low melting products enriched in P, S, etc. From the above result it is to note that solidification cracking associated with liquid during solidification occurred at columnar grain boundaries and migrated grain boundaries if the augmented-strain was large and that ductility-dip cracking occurred at migrated grain boundaries after solidification. Consequently, the crack along a migrated boundary could not be distinguish by light microstructure except for SEM microstructure of the crack surface. The subsequent sections will deal with the effect of impurities and the subsequent report will discuss for further details.

In case of SUS 316 the microstructure shows a negligible amount of δ-ferrite. Solidification cracks occurred predominantly along columnar grain boundaries as shown in Fig. 4 (d) and small ductility-dip cracks occurred along a migrated grain boundary as shown in Fig. 4 (e).

SUS 304 weld metal contained about 5% δ-ferrite as shown in Fig. 4 (f). A small solidification crack occurred along a columnar grain boundary. In case of SUS 321 and SUS 347 the length of solidification cracks was almost as long as that of SUS 304 weld metal. It should be noted, however, that a small content of δ-ferrite at room temperature displaced the role of the ferrite during solidification and subsequent cooling, as discussed in the previous report.

From the above-mentioned results, SUS 310S weld metal which shows the fully austenitic microstructure is the most susceptible to solidification and ductility-dip crackings. SUS 316 weld metal is sensitive to solidification cracking. SUS 304, SUS 321 and SUS 347 weld metals which contained some ferrite are less susceptible to solidification and ductility-dip crackings. These data were in accordance with the former reports[7] and the practical use.

3.2 Effect of phosphorus on hot crack susceptibility

The specimens which had been used to compare the difference of the segregation behaviour of phosphorus between SUS 310S and SUS 304 weld metals in the previous report[9] were again utilized to investigate the effect of the increasing P content on the hot crack susceptibility determined by the Trans-Varestraint test. The effect of P contents on the BTR and the ductility curves of SUS 304 and SUS 310S weld metals is shown in **Fig. 6**. In case of SUS 304 the P contents which were increased from about 0.02 to 0.1% showed a little influence on widening the BTR. It was the weld metal containing about 0.25% P that widened the BTR a little and dropped E_{min} considerably. Therefore, it is suggested that the detrimental effect of P on hot crack susceptibility is negligible in commercial SUS 304 weld metal containing δ-ferrite, probably because the segregation of P to grain boundaries may be reduced due to the primary solidification of the ferrite[9]. It was very difficult, in fact, to find out phosphides even in the weld metal containing 0.25% P as shown in **Fig. 7**. In case of SUS 310S the BTR

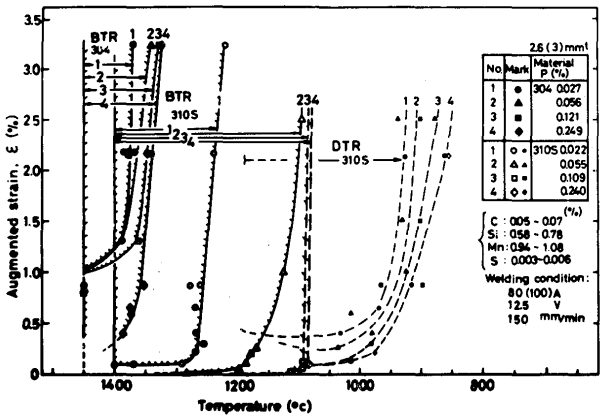

Fig. 6 Effect of increasing *P* contents on BTR and ductility curves of SUS 310S and SUS 304 weld metals.

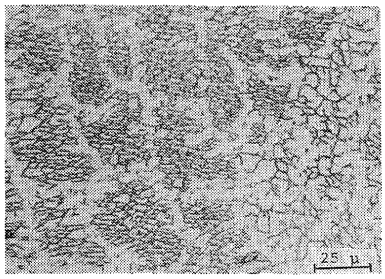

Fig. 7 Room temperature microstructure from SUS 304 weld metal containing about 0.25% *P*.

widened extensively and E_{min} lowered extremely when P contents were increased over 0.05% to weld metals. The light and electron microstructures, and the diffraction pattern and its key-diagram taken from inclusions from SUS 310S weld metal containing about 0.1% P are shown in **Fig. 8 (a)** to **(d)**. The SEM microstructure of residues electrolytically extracted and the analytical result with an energy dispersive X-ray spectrometer (EDX) are further shown in **Fig. 9**. The inclusions were identified as phosphides of the form M_3P and enriched in Cr and P especially. The residues electrolytically extracted were also identified as the austenite and the phosphide of the type M_3P with X-ray diffraction (XD) method. Therefore, an eutectic with a γ(Fe, Cr, Ni, Mn, etc.) solid solution and a phosphide of the type $(Cr, Fe, etc.)_3P$ must have been reasonably

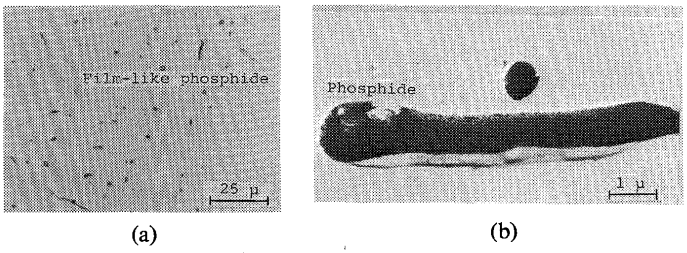

(a) (b)

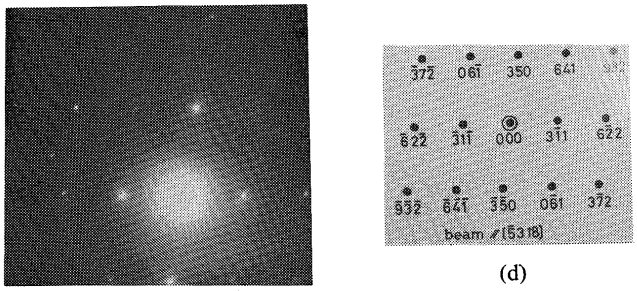

(c) (d)

Fig. 8 Light and electron microstructures (a), (b) and diffraction pattern (c) and its key-diagram (d) from inclusion in SUS 310S weld metal containing 0.1%P showing M_3P type phosphide.

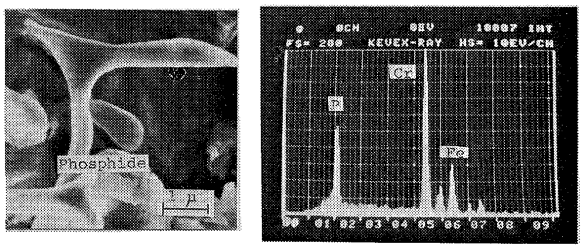

(a) (b)

Fig. 9 SEM microstructure of residue electrolytically extracted from SUS 310S weld metal containing 0.24%P showing its morphology (a) and analytical result of EDX showing enrichment of Cr and P in residue (b).

formed in grain boundaries. Phosphides of M_3P type were detected even in commercial SUS 310S weld metal containing about 0.02%P as well as the weld metal containing 0.1% P with ED and EDX of SEM. Although 0.1% P content in Fig. 8 (a) is an extreme case, film-like phosphides are observed along columnar grain boundaries. Subsequently the eutectic melting of phosphides was directly observed using the hot stage microscopy. The room temperature microstructure from SUS 310S cast ingot containing 0.24% P is shown in **Fig. 10 (a)**, which was observed at about 1100°C on a heating cycle in argon atmosphere by the hot stage microscope as shown in **Fig. 10 (b)**, and it gives evidence of melting behaviour of a phosphide. The eutectic melting of phosphide in SUS 310S weld metal containing from about 0.05 to 0.24% P was

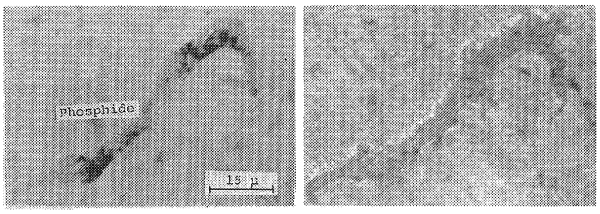

(a) (b)

Fig. 10 Room temperature microstructure of SUS 310S cast ingot containing 0.24%P (a) and microstructure at 1100°C on a heating cycle observed by hot stage microscope showing melting behaviour of eutectic with austenite and phosphide (b).

observed to occur at about 1060 to 1100°C as well as SUS 310S cast ingot. The melting point was accepted as corresponding to the lowest temperature of the BTR, actually the crack occurred within the BTR in case of the augmented strain below 0.1% and the melting point was higher than the lowest temperature of the DTR. From the above result it is suggested that the increase in P content is the most detrimental in SUS 310S weld metal and it is expected that the decrease in P content is beneficial mainly because the content of phosphides of low melting point decreases as well as the segregation of P to boundaries reduces. The effect of decreasing P conent in SUS 310S weld metal was again investigated in **Fig. 11**. The decrease in P content had a considerable influence on narrowing the BTR gradually, probably because the reduction in P content may result in a corresponding decrease in low melting products as well as higher bulk solidus temperature. In case of the lowest P content, hot cracking may be reduced since the Si content was fairly reduced in addition. However, SUS 310S containing lower P and Si would not achieve the good resistance of SUS 304 to hot cracking because low E_{min} was not raised.

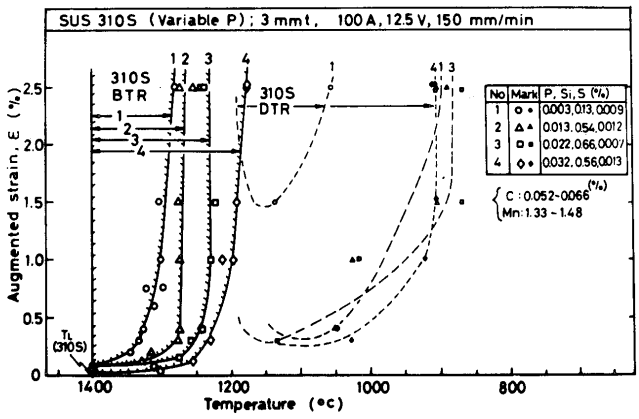

Fig. 11 Effect of decreasing P contents on BTR and ductility curve of fully austenitic SUS 310S weld metal.

3.3 Effect of sulphur on hot crack susceptibility

The specimens used in the previous report were examined to compare the effect of S on the hot crack susceptibility between SUS 304 and SUS 310S weld metals. The effect of S contents on the BTR and the ductility curves of SUS 304 and SUS 310S during welding is shown in **Fig. 12**. In case of SUS 304 the increase in S content widened the BTR appreciably

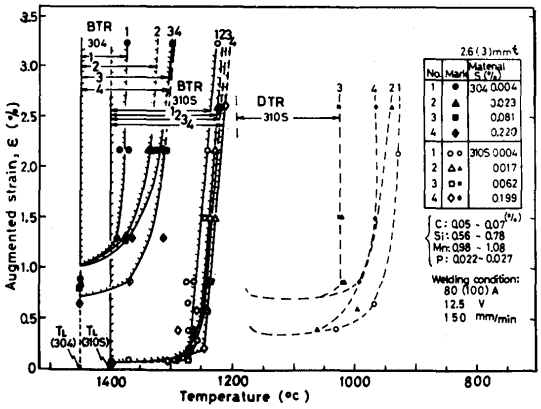

Fig. 12 Effect of increasing S contents on BTR and ductility curves of SUS 304 and SUS 310S weld metals.

and reduced the value of CST from 22×10^{-5} to 12×10^{-5} (1/°C). However, E_{min} was still raised, so that it is supposed that SUS 304 can be resistant to hot cracking even if the S content is increased to some extent. The residues electrolytically extracted from SUS 304 weld metal containing about 0.2% S are shown as an example in SEM microstructure of

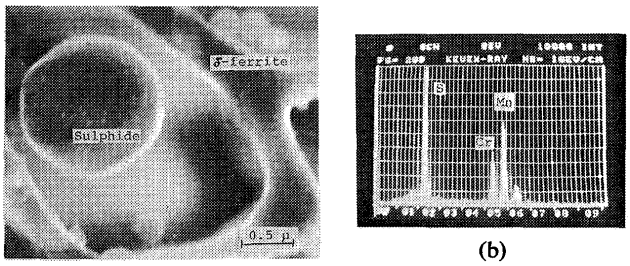

(a) (b)

Fig. 13 SEM microstructure of weld metal residue in SUS 304 containing 0.2%S (a) and analytical result of EDX of granular inclusion showing enrichment of Mn, Cr and S (b).

Fig. 13 (a) and the analytical result of a granular inclusion in Fig. 13 (a) by EDX is also shown in **Fig. 13 (b)**. The residues were subsequently analyzed by ED and XD. Inclusions were identified as sulphides of the form α-MnS by ED. Furthermore, the XD result obtained is shown in **Table 3**. These results indicate that SUS 304 weld metal containing about 0.2% S consisted mainly of austenite, α-ferrite and sulphides which were identified as the type α-MnS and enriched in Mn, Cr and S; the solubility of Cr in MnS was considerably large. The melting point of sulphides in the case of 0.2%S was directly observed with the hot stage microscope, so that it was about 1280 to 1310°C, which was almost similar to the lowest temperature of the BTR and was much lower with respect to the bulk solidus temperature of commercial SUS 304. Nevertheless, the E_{min} was still high, which must be influenced by the solidi-

Table 3 X-ray diffraction result observed with weld metal residues of SUS 304 containing 0.22% S.

d measured (Å)	Observed diffraction line relative intensity (CrKα)	ASTM Powder Data File			
		α-MnS (a=5.224Å) (CuKα)	ferrite (a=2.8664Å) (CuKα)	austenite (a=3.58Å)* (CrKα)	$Cr_{23}C_6$ (a=10.638Å) (CrKα)
2.58	100	3.015 (13) 2.612 (100)			2.37 (50)
2.07	50			2.067 (100)	2.17 (50) 2.05 (100)
2.02	100		2.0268(100)		
1.82	50	1.847 (48) 1.575 (6)		1.79 (50)	1.88 (50) 1.80 (50)
1.48	30	1.509 (19)			1.293 (60) 1.256 (100)
1.43	30		1.4332(20)		1.231 (90)
1.17	80	1.306 (8) 1.1682(19) 1.0662(15)	1.1702(30)	1.266 (70)	1.192 (80) 1.170 (90)

* W.P.Ress et al. (1949)162,325, & J.CooK etal. (1952)171,345 J. Iron and Steel Inst.

fication process and the morphology of liquid forming sulphides. The major effect of S was to widen the BTR appreciably due to its segregation.

In case of SUS 310S the increase in S content had a little influence on the BTR and the ductility curves. The electron microstructure, the diffraction pattern and its key-diagram taken from inclusions from SUS 310S weld metal containing about 0.2%S are shown in **Fig. 14**. Moreover, the SEM microstructure of the residue electrolytically extracted and the analytical result of the residue are shown in **Fig. 15**. The inclusion was identified as a sulphide of α-MnS type and was

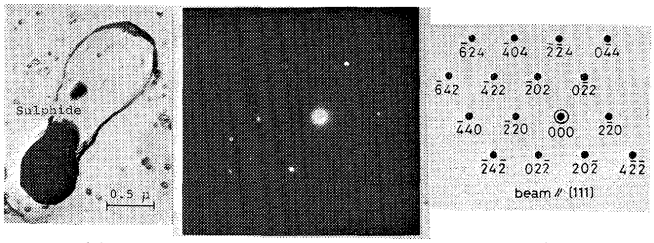

(a) (b) (c)

Fig. 14 Electron mecrostructure (a) and diffraction pattern (b) and its key-diagram (c) taken from inclusion in (a) in SUS 310S weld metal containing 0.2%S showing the presence of MnS.

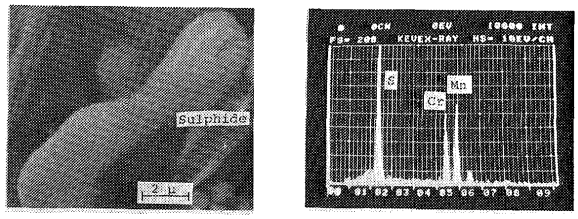

(a) (b)

Fig. 15 SEM microstructure of residue electrolytically extracted from SUS 310S weld metal containing 0.2%S (a) and analytical result of EDX of residue showing enrichment in Mn, Cr and S (b).

enriched in Mn, Cr and S. Sulphides of MnS type were detected even in the weld metal containing about 0.005%S. Subsequently, the melting point of a sulphide in the weld metal containing 0.2%S was directly observed with the hot stage microscope. The temperature was about 1260 to 1310°C and was higher than the lowest temperature of the BTR of SUS 310S weld metal. That is probably why the increase in S content hardly widened the BTR. Since granular sulphides formed finished solidifying at higher temperature of the BTR, the effect of S on the hot crack susceptibility must be slight. This result suggests that the effect of P may be substantial even in the commercial level (0.02%) of P content as well as the beneficial effect of Mn can reasonably be expected. The detrimental effect of S must become notable when the detrimental effect of P is diminished or the Mn content is reduced.

3.4 Effect of silicon on hot crack susceptibility

There is some evidence that Si increases hot cracking in fully austenitic stainless steel weld metal[4),14)]; detailed data are lacking, however. Moreover, since the element Si was likely to segregate to boundaries in fully austenitic SUS 310S as discussed in the previous report[9)], the Si content was decreased from about 1 to 0.1%. The effect of Si on the BTR and the ductility curves is shown in **Fig. 16**. The decrease in Si content from about 1 to 0.1% narrowed the BTR gradually from 165 to 110°C and E_{min} of the DTR was raised in case of 0.11% Si. That is probably because the segregation of Si to boundaries was decreased according to the decreasing Si content[18)]. The microstructure was fully austenitic.

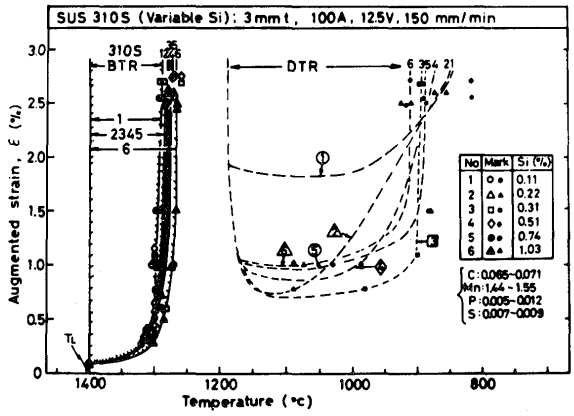

Fig. 16 Effect of decreasing Si contents on BTR and ductility curve of SUS 310S weld metal.

3.5 Effect of manganese on hot crack susceptibility

The beneficial effect of Mn was expected to reduce the detrimental effect of S in the previous section 3.3. Besides according to J. Honeycombe and T.G.Gooch[15)] the addition of between 2% and 6% Mn reduced cracking. Therefore, the Mn contents were varied from about 1 to 10.5%, based on the 25Cr-20Ni type alloy. The effect of Mn on the BTR and the ductility curves is shown in **Fig. 17**. The tendency of the ductility curves was not varied extensively between 1% and 10.5% Mn, except that the value of CST was a little lower in 10.5% Mn. The result shows that the beneficial effect of increasing Mn content expected on hot crack susceptibility was not notable probably because the S content contained in specimens was decreased in 0.003 to 0.005% in this investigation and consequently the cracking caused by S could be reduced considerably

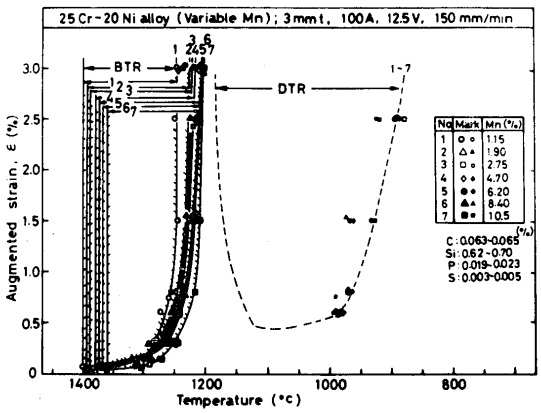

Fig. 17 Effect of increasing Mn contents on BTR and ductility curve of 25Cr-20Ni type weld metal.

by the addition of about 1% Mn and the effect of over 1% Mn was nearly neutral.

3.6 Effect of carbon on hot crack susceptibility

The increase in C content has been reported to be useful to reduce or prevent cracking[16] and 0.4C-25Cr-20Ni type (HK40) alloy has been generally acknowledged[17] to be less sensitive to hot cracking than SUS 310S. However, the details are not explained. The C content was increased from 0.07 to 0.53% in 25Cr-20Ni type alloy. The effect of C on the BTR and the ductility curves is shown in **Fig. 18**. As far as the

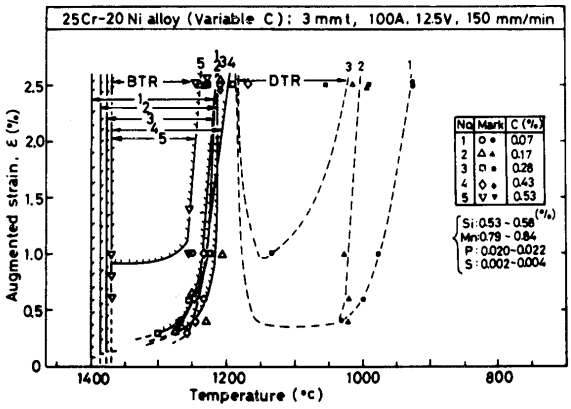

Fig. 18 Effect of increasing C contents on BTR and ductility curve of 25Cr-20Ni type weld metal.

solidification crack susceptibility is concerned, the weld metals containing from 0.07 to 0.43% C were not varied in the tendency of the ductility curves, except that the weld metal containing 0.53% C exhibited the narrower BTR and the higher E_{min}. The DTR was narrowed considerably and the E_{min} of the DTR was raised according to the increase in C content. The light and electron microstructures and the diffraction pattern from inclusions from the weld metal containing 0.28%

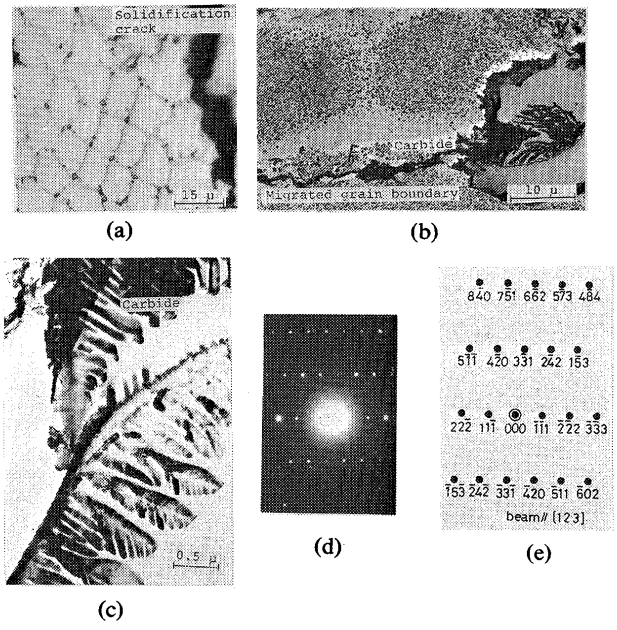

Fig. 19 Light and Electron microstructures (a) (b) (c) of 0.28%C-25Cr-20Ni weld metal and diffraction pattern (d) taken from black phase and its key-diagram (e) showing $M_{23}C_6$ type carbide.

C are shown in **Fig. 19** (**a**) to (**e**). The microstructure in Fig. 19 (a) shows a solidification crack and the presence of another phase at boundaries appreciably. Fig. 19 (b) and (c) shown in higher magnification exhibits the dendritic phase to form a mass and to precipitate along a migrated grain boundary. The phase was identified as a carbide of the form $M_{23}C_6$ (M is predominantly Cr). The light and electron microstructures from the weld metals containing 0.43% C and 0.53% C and the diffraction pattern from inclusions at boundaries in 0.53C-25Cr-20Ni weld metal and its key-diagram are shown in **Fig. 20** (**a**) to (**f**). The XD result from 0.53%C weld metal is further shown in **Fig. 21**. Eutectics, part of which were identified as carbides of the form M_7C_3 were formed along cellular dendritic and columnar grain boundaries in the percent of about 7 and 11.5 in area in case of 0.43% C and 0.53% C weld metals respectively. That is to say, the microstructures show two types of carbides. In case of C content till 0.28%, carbides of the form $M_{23}C_6$ were formed along migrated grain boundaries during cooling after solidification and in case of 0.43 and 0.53% C M_7C_3 carbides were formed as part of eutectics with γ solid solution and (Cr, Fe, etc.)$_7C_3$ along cellular dendritic and columnar grain boundaries during solidification. The γ-M_7C_3 eutectic temperature was about 1275°C from the thermal analysis using a crucible and about 1270 to 1280°C from the direct observation by the hot stage microscope. The temper-

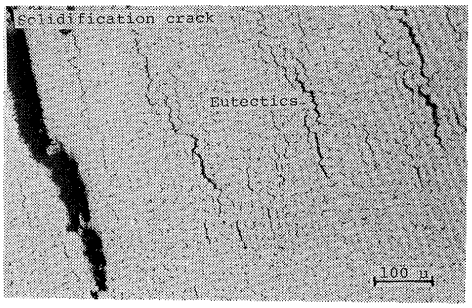

(a)

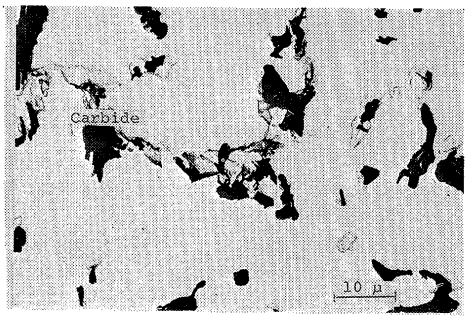

(b)

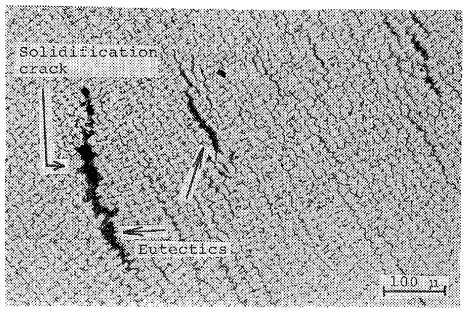

(c)

(d)

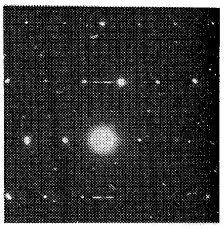

(e)

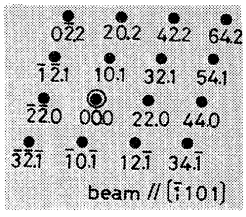

(f)

Fig. 20 Light and Electron microstructures of 0.43%C-25Cr-20Ni (a) (b) and 0.53%C-25Cr-20Ni weld metals (c), (d) and diffraction pattern taken from black phase (e) and its key-diagram (f) in 0.53% C-25Cr-20Ni weld metal showing evidence of M_7C_3 carbide.

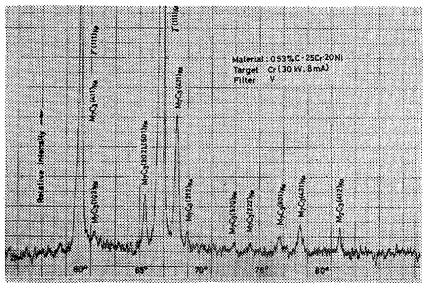

Fig. 21 X-ray diffractometer result on weld metal containing 0.53%C showing presence of M_7C_3 carbide.

ature measured corresponded to the lowest temperature of the BTR of the weld metal containing 0.53%C. In the columnar grain boundaries of the weld metals containing 0.43 and 0.53% C where the solidification cracks occurred or if not when the strain was applied by the Trans-Varestraint test thicker eutectics existed as shown in 19 (a) and 19 (c). This phenomenon was observed as if the area of the thick eutectics could have been healed. The weld metal showing considerable amounts of eutectics may be resistant to hot cracking.

4. Conclusion

(1) The hot crack susceptibility of weld metals of commercial austenitic stainless steels was investigated using the Trans-Varestraint test. Fully austenitic SUS 310S exhibited the widest BTR from about 1400 to 1240°C and the widest DTR from about 1200 to 850°C. Duplex austenitic SUS 304 exhibited the narrowest BTR from about 1430 to 1370°C and no DTR. Consequently it can be easily understood that SUS 310S is the most susceptible to hot cracking, in particular, solidification cracking, due to the lowest E_{min} in addition to the widest BTR, and that SUS 304, etc. containing δ-ferrite are resistant to hot cracking. The commercial stainless steels investigated are rated in decreasing order of hot crack susceptibility as follows: SUS 310S, SUS 316, SUS 347, SUS 321 and SUS 304.

(2) In case of SUS 304 the detrimental effect of the increasing P content was slight because the segregation of P to boundaries was much smaller due to the primary solidification of δ-ferrite in comparison with the primary solidification of the austenite in SUS 310S. In case of SUS 310S showing fully austenitic microstructure the detrimental effect of the increasing P content was understood from viewpoint that the increase in P content widened the BTR gradually and dropped the value of E_{min}, because P was likely to segregate to form low melting eutectics with γ and M_3P phosphides in boundaries. Since the decrease in P content from a commercial level of 0.02 or 0.03%

affected the reduction of the BTR, the P content should be further reduced to improve the hot crack susceptibility. However, the weld metal containing 0.003% P cannot yet achieve the resistance of SUS 304 to hot cracking.

(3) In case of SUS 304 the detrimental effect of the increasing S content was to widen the BTR slightly. However, it is appreciated that solidification cracking was unlikely to occur because E_{min} was higher and CST was larger in comparison with commercial SUS 310S even if the weld metal contained about 0.2%S. In case of SUS 310S the detrimental effect of the increasing S content on the BTR and the ductility curves was slight, probably because sulphides were formed in the morphology of granular α-MnS at higher temperature than the lowest temperature of the BTR.

(4) Since the decrease in Si content narrowed the BTR a little but did not raise E_{min}, the effect of decreasing Si content was expected a little.

(5) The beneficial effect of between 1% and 10.5% Mn on hot cracking was not notable from the results determined from the BTR and the ductility curves, as the S content was 0.003 to 0.005%.

(6) The increase in C content from 0.07 to 0.43% did not vary the BTR but narrowed the DTR considerably. Since the more addition of C content to 0.53% narrowed the BTR, raised E_{min} of the BTR extremely and moreover diminished the DTR, the weld metal containing about 0.5% C were reasonably expected to resistant to hot cracking. However, unfortunately it was not fully austenitic but consisted of the austenite (γ) and eutectics with γ and M_7C_3 carbides. The content of the eutectics was about 11.5% and consequently it is considered that the formation of considerable amounts of eutectics is necessary and beneficial to reduce cracking. Meanwhile, carbides formed in case of the addition of between 0.07 and 0.28% C were mainly $M_{23}C_6$ carbides which predominantly all over migrated boundaries. The increase in carbides according to the increasing C content restricted the mobility of grain boundaries and improved the ductility-dip tendency.

Acknowledgements

The authors wish to thank the work of Professor T. Enjyo and Dr. S. Nasu of JWRI for the co-operation of EM method and Mr. T. Uehara, the graduate student of the Welding department of Osaka University, for co-operation of electrolytical extraction and XD methods, and acknowledge Mr. S. Saruwatari of Nippon Steel Corporation and Mr. K. Saito of Nippon Stainless Steel Corporation for their supplying materials used.

References

1) J. C. Borland and R. D. Younger: "Some Aspect of Cracking in Welded Cr-Ni Austenitic Steels", Brit. Weld. J., Vol. 7 (1960), pp 22–59.
2) I. Masumoto, et al.: "Hot Cracking of Austenitic Steel Weld Metal", J. Japan weld. Society, Vol. 41 (1972) No. 11 pp. 1306–1314. (in Japanese)
3) P. W. Jones: "A Summary of Recent Work on the Murex Hot Cracking Test", Brit. Weld. J., Vol. 4 (1957), pp. 189–197.
4) F. C. Hull: "Effect of Alloying Additions on Hot Cracking of Austenitic Chromium-Nickel Stainless Steels", Pro. Amer. Soc. for Testing and materials, 60 (1960), pp. 667–690.
5) F. C. Hull: "Effect of Delta Ferrite on the Hot Cracking of Stainless Steel", Weld. J., (1967), pp. 399s–409s.
6) K. Saito, et al.: J. Japan Weld. Society, Vol. 40 (1971) pp. 1178–1180. (in Japanese)
7) C. D. Lundin, W. T. DeLong and D. F. Spond: "Ferrite-Fissuring Relationship in Austenitic Stainless Steel Weld Metals", Weld. J. Vol. 54 (1975), pp. 241s–246s.
8) Y. Arata, F. Matsuda and S. Saruwatari: "Varestraint Test for Solidification Crack Susceptibility in Weld Metal of Austenitic Stainless Steels", Trans. JWRI, Vol. 3 (1974), No. 1, pp. 79–88.
9) Y. Arata, F. Matsuda and S. Katayama: "Solidification Crack Susceptibility in Weld Metals of Fully Austenitic Stainless Steels (Report I)", Trans. JWRI, Vol. 5 (1976) No. 2, pp. 135–151.
10) B. Hemsworth, T. Boniszewski and N. F. Eaton: "Classification and Definition of High Temperature Welding Cracks in Alloys", Metal Const. & Brit. Weld. J., (1969), Feb., pp. 5–16.
11) G. L. Petrov and V. N. Zemzin: "Influence of Ferrite on the Crystallisation of Austenitic Weld Metal and the Formation of Hot Cracks during Welding", Svar. Prioz., (1967), No. 2, pp. 1–3.
12) T. Senda, F. Matsuda et al.: "Studies on Solidification Crack Susceptibility for Weld Meatls with Trans-Varestraint Test (2)", J. Japan Weld. Soc., Vol. 41 (1972), No. 6, pp. 709–723 (in Japanese)
13) Y. Arata, F. Matsuda, K. Nakata and I. Sasaki: "Solidification Crack Susceptibility of Aluminum Alloy Weld Metals (Report I)", Trans. JWRI, Vol. 5, (1976), No. 2, pp. 153–167.
14) S. Polgary: "The Influence of Silicon Content on Cracking in Austenitic Stainless Steel Weld Metal with Particular Reference to 18Cr-8Ni Steel", Metal Const. & Brit. Weld. J., (1969) Feb. pp. 93–97.
15) J. Honeycombe and T. G. Gooch: "Effect of Manganese on Cracking and Corrosion Behavior of Fully Austenitic Stainless Steel Weld-Metals", Metal Const. & Brit. Weld. J., (1972) Dec. pp. 456–460.
16) D. M. Hadrill and R. G. Baker: "Microcracking in Austenitic Weld Metal", Brit. Weld. J., (1965) Aug. pp. 411–419.
17) I. Ono et. al., "The Effect of Carbon Content on Some Properties of 25Cr-20Ni Cast Steel for Reformer Tube", Report for Japan Stainless Steel Corporation. (in Japanese)
18) Unpublished research at Welding Research Institute, Osaka.